Available online at www.sciencedirect.com
SCIENCE DIRECT
Microporous and Mesoporous Materials 91 (2006) 187–195
MICROPOROUS AND MESOPOROUS MATERIALS
www.elsevier.com/locate/micromeso

Effect of zeolite geometry for propane selective oxidation on cation electrostatic field of Ca^{2+} exchanged zeolites

Jiang Xu, Barbara L. Mojet, Leon Lefferts *

Catalytic Processes and Materials, Faculty of Science and Technology, Institute of Mechanics Processes and Control Twente (IMPACT), University of Twente, P.O. Box 217, 7500 AE Enschede, The Netherlands

Received 13 July 2005; received in revised form 18 November 2005; accepted 22 November 2005
Available online 18 January 2006

Abstract

The effects of zeolite geometry on propane selective oxidation were studied by in situ infrared spectrometry on Ca^{2+} exchanged Y, MOR and ZSM5 zeolites. Oxygen and propane adsorption at room temperature, revealed that the electrostatic field of Ca^{2+} increased in the order CaY < CaMOR < CaZSM5. The electrostatic field of Ca^{2+} cations in CaY and CaZSM5 was observed to correlate with propane selective oxidation activity and selectivity. At 353 K, low activity but high selectivity to acetone was observed for propane oxidation on CaY zeolite, while high activity and a 2:1 mixture of 2-propanol and acetone was observed on CaZSM5. CaMOR showed the lowest activity for oxygenates formation of propane oxidation, but deep oxidation to CO and CO_2 was found. The results convincingly show that the geometrical structure of a zeolite determines activity and selectivity of propane partial oxidation on Ca^{2+} exchanged zeolites to a large extent.

Keywords: Propane; Electrostatic field; Zeolite; Geometry; Selective oxidation

1. Introduction

Recently, a new approach of photo as well as thermal selective oxidation of alkanes at low temperature on alkali or alkaline-earth exchanged Y zeolite was presented, and initiated a new branch of research in the field of hydrocarbon partial oxidation processes [1–7]. It was proposed that the reaction involved the formation of an ion pair of hydrocarbon and oxygen ($C_nH^+_{2n+2}O^-_2$), which is stabilized in the electrostatic field of cation-exchanged Y zeolite. The alkyl hydroperoxide is produced from this charge transfer state and further goes on to form carbonyl containing product exclusively by elimination of water. The high activity and selectivity of this reaction was suggested to depend on both the electrostatic field at the cation site and the dynamics of the reactant molecules within the confined zeolite structure. Therefore, the zeolite structure, the framework composition, and the properties of the charge compensating cations are parameters that can be expected to impact catalytic activity and selectivity in zeolite catalyzed selective oxidation of alkanes.

Barium exchanged X, Y, ZSM5 and Beta have been used to investigate photo-oxidation of 1-alkenes, toluene and *p*-xylene [2,6]. However, selectivity was found to dramatically decrease in the order X > Y > Beta > ZSM5, which was attributed to the presence of residual Brönsted acid sites in these zeolites. The results also revealed that shape selectivity played an important role in determining product selectivity in condensation side reactions [6].

Nevertheless, no results have been published for the influence of the zeolite host for the thermally activated alkane oxidation on cation-exchanged zeolites. Experimental results of CO adsorption showed that the electrostatic field increased with divalent cations versus monovalent cations for a given zeolite host, and for a given cation increased for zeolites with higher Si/Al ratios [2,6]. In our previous work, we have systematically investigated thermal

* Corresponding author. Tel.: +31 53 4892858; fax: +31 53 4894683.
E-mail address: l.lefferts@utwente.nl (L. Lefferts).

1387-1811/$ - see front matter © 2005 Elsevier Inc. All rights reserved.
doi:10.1016/j.micromeso.2005.11.040

selective oxidation of propane to acetone on alkaline-earth exchanged Y zeolite [1,8]. The results have convincingly shown that activity and selectivity of propane oxidation to acetone are influenced not only by the charge/radius ratio (intrinsic electrostatic field) of earth-alkali cations [1], but also by the cation location and the Brönsted acidity of Y zeolite [8]. So if oxidation of hydrocarbons in zeolites is a general phenomenon, then the shape and size of zeolites may potentially be used to better control activity and selectivity of the thermal propane selective oxidation reaction.

In this work, we have investigated three types of Ca^{2+} exchanged zeolites: mordenite and ZSM5, in addition to Ca^{2+} exchanged Y zeolite. Zeolite Y is the synthetic form of faujasite and has a Si/Al ratio between 2 and 5. Its three-dimensional framework has two main cages: the large supercage results from an assembly of the basic units, the sodalite cages (Fig. 1a). The spherical supercages are approximately 1.3 nm in diameter. Access to the supercages is afforded by four 12-membered ring windows about 0.74 nm in diameter, which are tetrahedrally distributed around the center of the supercages. Cations can occupy three positions in Y zeolite (see Fig. 1a). The first type, sites I and I′, is located on the hexagonal prism faces between the sodalite units. The second type, sites II′ and II, is located in the open hexagonal faces. The third type, site III, is located on the walls of the supercage. ''Large pore'' mordenite is a one-dimensional zeolite consisting of main channels parallel to the [0 0 1] crystal plane. The channels have a lightly elliptical cross section of a 12-membered ring with a diameter of 0.7×0.65 nm (Fig. 1b). Single crystal refinement of dehydrated NaMOR has revealed five different sites for cation location (see Fig. 1b) [9]. The occupation of the cations in the five types of sites depends on the Si/Al ratio. For MOR with Si/Al ratio of 10, each unit cell contains three sodium cations located at site I (in side channel) and two sodium cations occupying site IV (in the intersection between eight-ring and main channel). Zeolite ZSM5 with medium pore sizes is characterized by a two-dimensional pore system with straight, parallel channels intersected by zigzag channels (Fig. 1c, the detailed 3D structure can be found on the website: http://www.iza-structure.org/databases/). Both channels consist of 10-membered rings with a diameter of 0.53×0.56 nm (straight channels) and 0.51×0.5 nm (sinusoidal channels). IR studies of H_2 and CO adsorption indicated that the cations are preferentially located at the intersections of the sinusoidal and straight channels at the edge of a four-membered ring (site I) [10,11]. Additionally, small cations, like Na^+ are also found in small cavities above the sinusoidal channel (site II), but MAS-NMR studies showed a low occupancy of this site (10%) (Fig. 1c) [12].

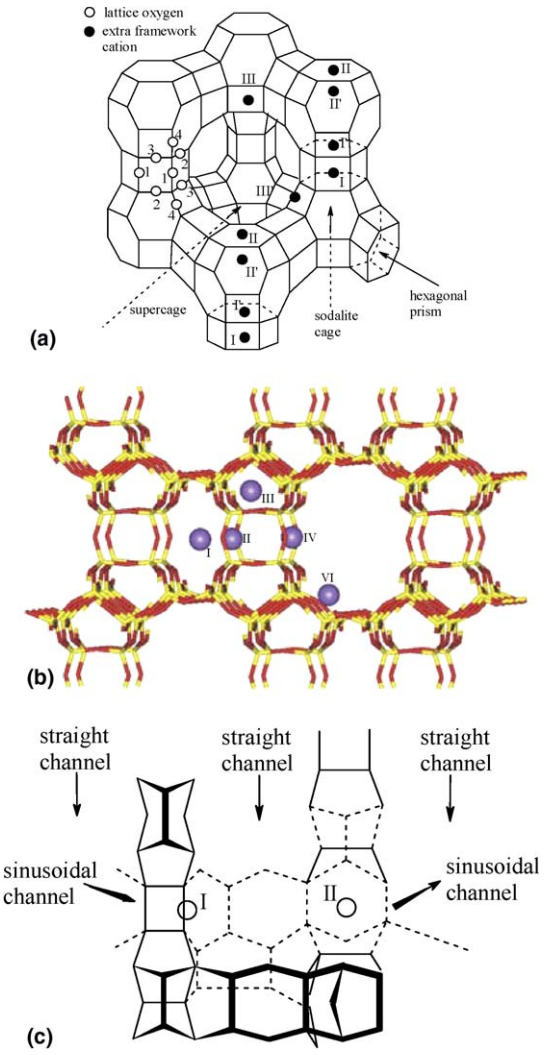

Fig. 1. Framework structure with cation sites indicated of (a) Y zeolite, (b) mordenite (MOR), (c) MFI (ZSM5) (view of the [1 0 0] plane).

Up to now, the partial oxidation of alkanes over cation-exchanged zeolites mainly focused on the surface reaction, since the products are strongly adsorbed, and therefore the catalytic cycle has not been closed yet. Nevertheless, this approach offers the unique opportunity to deeply investigate the activation of the involved molecules. Propane selective oxidation on CaY zeolite at room temperature showed that Ca^{2+} in the supercage (site II) provided the specific adsorption geometry to invoke reaction [8,13]. Slightly increasing Brönsted acidity could enhance reaction activity, but induced lower selectivity to acetone due to a minor amount of 2-propanol formation. In the present study, the activity and selectivity of the surface reaction of thermal propane oxidation in Ca^{2+} exchanged MOR and ZSM5 zeolites were compared with CaY by infrared spectroscopy to resolve the effects of zeolite geometry and Si/Al ratio on the selective propane oxidation mechanism.

2. Experimental

2.1. Materials

Zeolites CaY, CaMOR and CaZSM5 were prepared from respectively NaY (Zeolyst), NH_4MOR (Zeolyst), NH_4ZSM5 (Zeolyst). The parent zeolites were exchanged

Table 1
Zeolite chemical composition (determined by XRF)

Zeolite[a]	Chemical composition (wt.%)				Molar ratio			
	Na_2O	Al_2O_3	SiO_2	CaO	Si/Al	Na^+/Al	Ca^{2+}/Al	NH_4^+/Al[b]
CaMOR	0	7.31	88.66	3.14	10	0	0.39	0.22
CaY	1.087	21.76	65.99	11.12	2.6	0.08	0.47	–
CaHZSM5(38)	0	2.18	96.84	0.91	38	0	0.38	0.24
CaZSM5(25)	0.03	3.32	95.32	1.29	25	0.01	0.35	0.29

[a] CaY sample was prepared from NaY. CaZSM5 and CaMOR samples were prepared from respectively NH_4ZSM5 and NH_4MOR.
[b] NH_4^+ content was calculated based on the charge balance.

three times with 0.1 M solution of calcium nitrate (Merck) for 20 h at 363 K under stirring. The resulting cation-exchanged zeolites were washed three times with distilled water, filtered and dried overnight at 373 K. This resulted in the final form of CaY. The final form of CaMOR and CaZSM5 were obtained by calcination at 773 K under vacuum to decompose incompletely exchanged NH_4^+ ions. The chemical compositions of catalysts (determined by X-ray fluorescence (XRF)), Ca^{2+}/Al and NH_4^+/Al ratio, as well as sample names are listed in Table 1.

2.2. Infrared spectroscopy studies

The zeolite powder (30 mg) was pressed into a self-supporting wafer and analyzed in situ during adsorption and reaction by means of transmission FTIR spectroscopy using a Bruker Vector22 FTIR spectrometer with a MCT detector. A miniature cell, equipped with NaCl transparent windows, which can be evacuated to pressures below 10^{-7} mbar was used for the in situ experiments. The temperature is variable from room temperature to 773 K. Each spectrum consists of 32 scans taken at 4 cm^{-1} resolution.

The samples were activated in vacuum ($<10^{-7}$ mbar) at 773 K (ramp 10 K/min) for 2 h, subsequently cooled down to 473 K (dwell 10 h), and cooled to room temperature (294 K). Loading of reactants (propane and oxygen) was controlled by gas pressure. Propane was introduced into the IR cell until equilibrium was reached at 1 mbar in the gas phase, followed by addition of 40 mbar of oxygen. A calibration curve was made by adsorption of known amounts of acetone and 2-propanol at room temperature in order to determine the quantity of produced acetone and 2-propanol from propane and oxygen. The FTIR spectra were corrected for absorption of the activated zeolite.

3. Results

3.1. Catalyst characterization

Calibrated transmission FTIR spectra of the activated calcium exchanged zeolites are presented in Fig. 2. All samples showed an isolated silanol peak at 3740 cm^{-1} (ZSM5) and 3744 cm^{-1} (Y and MOR), which is either on the outer surface terminating the zeolite crystals or on silica impurities [14,15]. Bridging hydroxyl groups (SiOHAl groups,

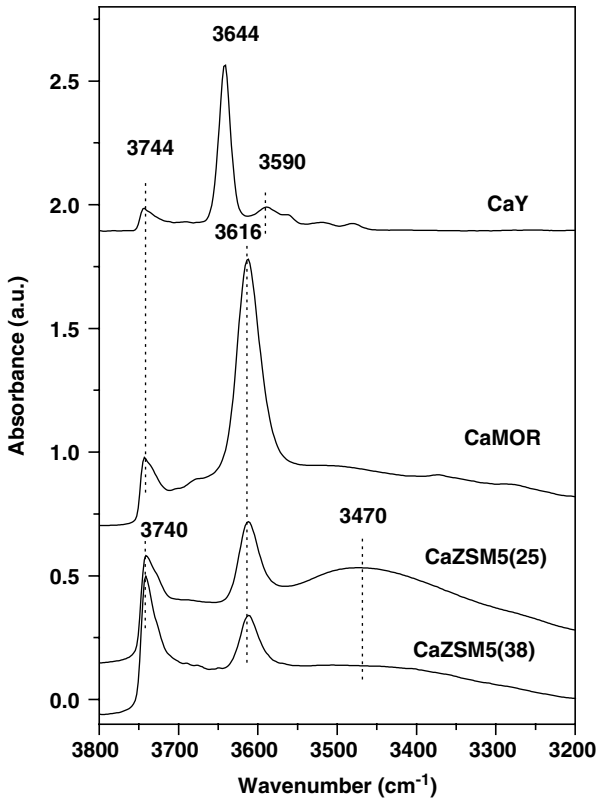

Fig. 2. Calibrated infrared spectra of Ca^{2+} exchanged Y, MOR and ZSM5 zeolites.

Brönsted acid sites) gave rise to IR absorption at 3644 cm^{-1} (Y), 3616 cm^{-1} (MOR) and 3616 cm^{-1} (ZSM5). High Brönsted acid site concentration was observed on CaMOR zeolite. For CaZSM5(38) the lowest amount of Brönsted acid sites was observed. The origin of Brönsted acid sites in these zeolites is twofold. First, due to incomplete exchange by Ca^{2+} cation for MOR and ZSM5 (see Table 1), the NH_4^+ in the parent zeolite is converted to H^+ during calcination. Second, hydrolysis of water at the Ca^{2+} sites during activation also result in some acidity, according to

$$Ca^{2+} + H_2O(ad) + Si\text{–}O\text{–}Al \rightarrow Ca(OH)^+ + Si\text{–}O(H^+)\text{–}Al$$

This reaction is thought to occur during activation at elevated temperature (for all studied zeolites) [1,14,15]. The hydroxyl vibration at 3590 cm^{-1} for CaY results from

$Ca(OH)_x$ species [1]. However, no $Ca(OH)_x$ species could be observed on CaMOR and CaZSM5, most likely due to the fact that this small peak is masked by the nearby high intensity hydroxyl vibration of Brönsted acid sites at 3616 cm^{-1}.

On ZSM5, a very broad band with maximum intensity around 3470 cm^{-1} belongs to perturbed hydroxyl groups that result from the presence of hydrogen bonding between OH groups and zeolite lattice oxygen [15].

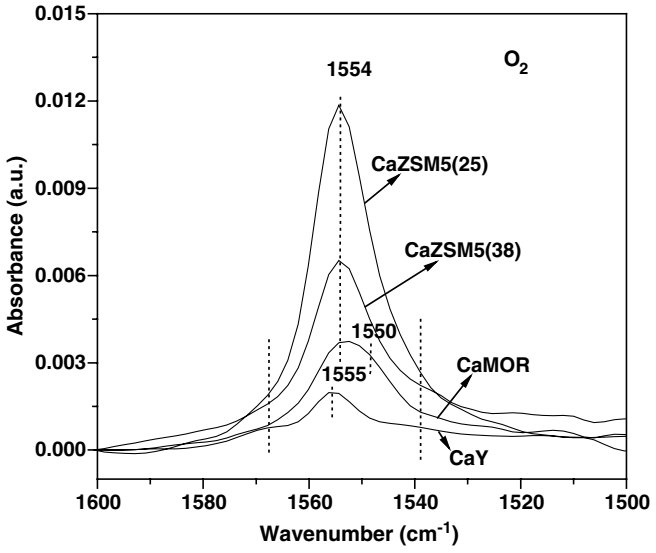

Fig. 3. Calibrated infrared spectra of room temperature oxygen adsorption at 40 mbar on Ca^{2+} exchanged zeolites.

3.2. Oxygen adsorption

Fig. 3 shows the room temperature infrared absorption of O_2 in Ca^{2+} exchanged Y, MOR and ZSM5 zeolites at 40 mbar O_2 equilibrium pressure after subtraction of the zeolite contribution to the spectrum. Clear broad bands appeared at 1554 cm^{-1} (CaZSM5), 1555 cm^{-1} (CaY) and 1554–1550 cm^{-1} (MOR), which can be attributed to the O–O stretch vibration in adsorbed O_2 [16–18]. High intensity of this band was found for CaZSM5(25), while with higher Si/Al ratio of CaZSM5(38), intensity slightly decreased. On CaMOR this oxygen stretch vibration band showed an asymmetric shape, which is composed of two peaks located at 1554 cm^{-1} and 1550 cm^{-1}. The peak intensity at 1554 cm^{-1} is slightly bigger than at 1550 cm^{-1}.

Further, two small side bands of adsorbed oxygen species were also found at high frequency side (about 1570 cm^{-1}) and low-frequency side (about 1542 cm^{-1}) on the studied Ca^{2+} exchanged zeolites. No changes could be observed in the OH-stretch region or other parts of the IR spectra after oxygen adsorption.

3.3. Propane adsorption

Fig. 4 displays the infrared spectra of propane adsorption on Ca^{2+} exchanged zeolites as function of propane partial pressure in the C–H stretch vibration range (3100–2600 cm^{-1}). Two main bands at 2970 cm^{-1} (methyl asymmetric stretching) and 2838 cm^{-1} (methyl symmetric stretching) were observed for propane adsorbed on CaY [19–21]. Both band intensities steadily increased with increasing propane partial pressure. On CaMOR and

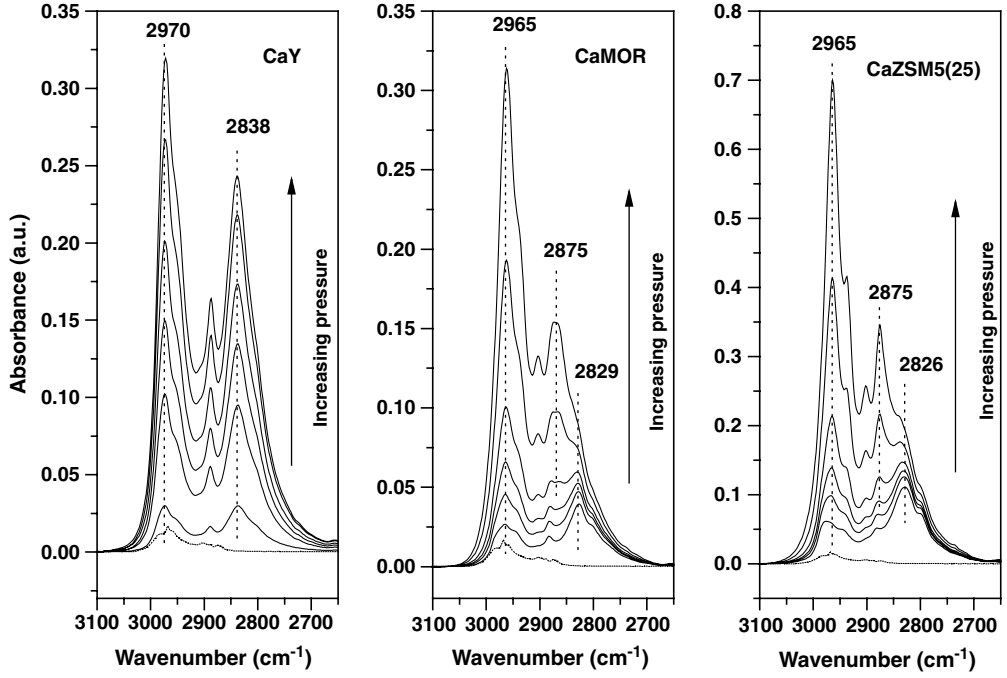

Fig. 4. Calibrated infrared spectra of room temperature propane adsorption on Ca^{2+} exchanged zeolites with equilibrium propane partial pressure of 0.01, 0.05, 0.1, 0.2, 0.5 and 1 mbar. Dot line shows 1 mbar propane in gas phase.

CaZSM5, at propane partial pressure below 0.2 mbar, two main bands at 2965 cm^{-1} (both CaMOR and CaZSM5(25)), and 2829 cm^{-1} (CaMOR) or 2826 cm^{-1} (CaZSM5(25)) were found and both increased in intensity with increasing propane partial pressure. With further increasing propane partial pressure the band intensities at 2829 cm^{-1} (CaMOR) and 2826 cm^{-1} (CaZSM5) did not vary significantly, however, an additional band at 2875 cm^{-1} was observed. With increasing propane partial pressure, this peak increased together with the high frequency band at 2965 cm^{-1}.

For CaZSM5(38) similar trends were observed, however with lower intensities at a given propane partial pressure (not shown).

Adsorption of propane only slightly disturbed the bridging hydroxyl groups (SiOHAl groups, Brönsted acid sites) at 3644 cm^{-1} (Y), 3616 cm^{-1} (MOR) and 3616 cm^{-1} (ZSM5), which has been discussed in detail in a previous paper [13].

3.4. Propane oxidation

Upon loading 1 mbar propane and 40 mbar oxygen on activated Ca^{2+} exchanged zeolites at 353 K, reaction was observed by following depletion of propane (band between 3010 and 2600 cm^{-1}) and production of acetone (band at 1682 cm^{-1}) and water (band at 1634 cm^{-1} (CaY), 1640 cm^{-1} (CaZSM5) and 1627 cm^{-1}(CaMOR)) (for experiment details see Refs. [1,8]). It should be noted that due to its weaker adsorption, the oxygen O–O band is very weak. Consequently, after co-adsorption of propane the band is masked by the strong IR band of propane at 1470 cm^{-1}, even though oxygen is presence in large excess [17]. Fig. 5 presents the infrared spectra after 20 h reaction at 353 K. It is clear that acetone formation increased in the order CaMOR < CaZSM5 < CaY. In addition to acetone and water, CO_2 and CO were found on CaMOR. From the infrared band structure it is clear that both CO and CO_2 are trapped inside the CaMOR zeolite, since two single sharp bands appear near 2215 cm^{-1} (CO) and 2365 cm^{-1} (CO_2) in the infrared spectra. The vibrational band structure normally found for gas phase CO and CO_2 is not observed. Also no CO_x or other products were found in the gas phase by online mass spectrometry for any of the zeolites. Further, no CO_x formation could be detected for CaY and CaZSM5 zeolites at all in either gas or solid phase.

After 20 h reaction, the systems with different zeolites were evacuated for 5 min to remove excess propane and oxygen. During evacuation, no acetone or 2-propanol were detected by on-line MS analysis. The infrared spectra afterwards are presented in Fig. 6. Clearly bands can be observed between 3100–2700 cm^{-1} and 1500–1300 cm^{-1}, which were previously masked by the intensive bands of propane C–H vibration and deformation. The bands at 3014, 2925, 1420 and 1379 cm^{-1} can be attributed to acetone [1]. The frequencies at 2989 cm^{-1} for CaY (Fig. 6a), 2981, 2943, 2887, 1462 and 1385 cm^{-1} for CaZSM5 (Fig. 6b and c) match the bands of 2-propanol, which was confirmed by comparing the infrared spectra of 2-propanol loaded on the corresponding zeolites. On CaMOR, a small amount of propane is still left (band at 2965 and 2829 cm^{-1}, about 5% of total adsorbed propane before evacuation), even after evacuation for 30 min (Fig. 6d). The intensity of CO (2215 cm^{-1}) and CO_2 (2365 cm^{-1}) on CaMOR decreased with evacuation (not shown).

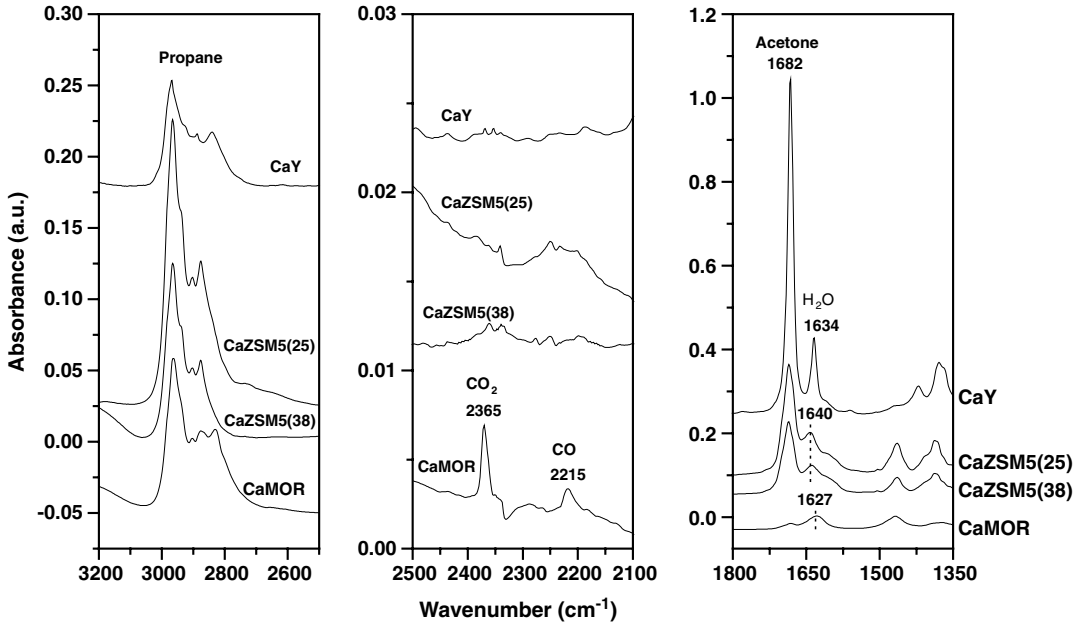

Fig. 5. Calibrated infrared spectra after 20 h propane oxidation at 353 K on Ca^{2+} exchanged zeolites.

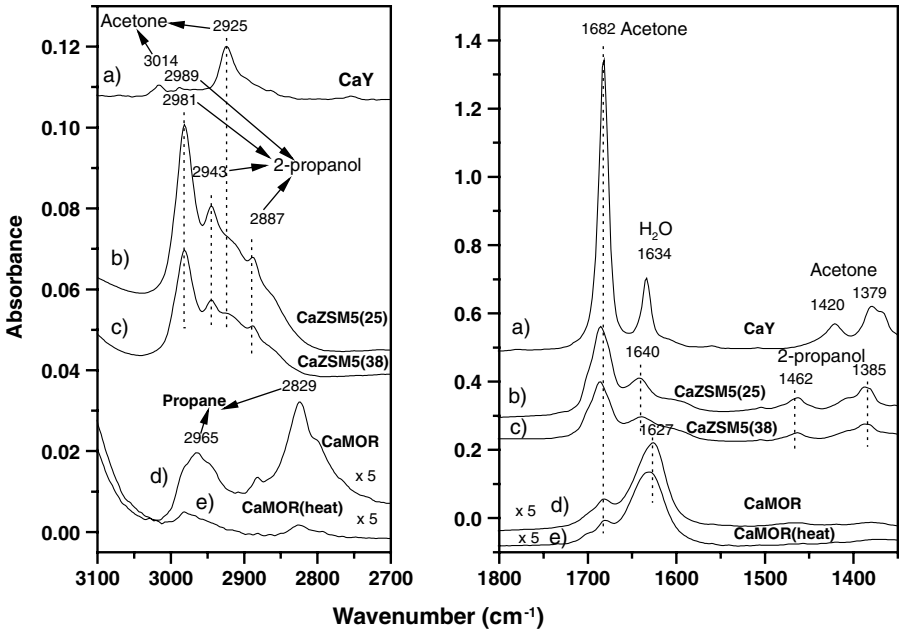

Fig. 6. Calibrated infrared spectra (a–d) after 20 h propane oxidation at 353 K on Ca^{2+} exchanged zeolites and subsequent evacuation for 5 min; (e) after (d), evacuated 30 min and followed heating to 423 K on CaMOR.

Evaluation of both intensities showed that about 30% of CO_2 and 15% CO desorbed after evacuation for 30 min. The CaMOR sample was then further heated to 423 K in vacuum (Fig. 6e). Clearly, during this treatment propane desorbed as well as CO and CO_2 (not shown). No additional bands were observed within the noise level.

After 20-h reaction at 353 K, lower acetone to water ratio was found on CaMOR than on CaY and CaZSM5 based on the infrared intensity of water (band at 1627–1640 cm^{-1}) and acetone (band at 1682 cm^{-1}). The amounts of acetone and 2-propanol produced on all zeolites after 20 h reaction are listed in Table 2. High selectivity to acetone was found on CaY, while a 2:1 mixture of 2-propanol and acetone was observed on both CaZSM5(38) and CaZSM5(25) zeolites. Only 3% of acetone was produced on CaMOR compared to CaY. Further, the amounts of produced water on the different samples (Fig. 5) also showed that much less propane was converted on CaMOR compared to CaY and CaZSM5.

Table 2
Propane oxidation at 353 K on Ca^{2+} exchanged zeolites

Zeolite	Products (μmol/g)		ol/one	(one + ol)/Ca^{2+} (molar ratio)
	Acetone	2-Propanol		
CaMOR	4.4	–	–	0.02[a]
CaY	146.9	1.4	0.01	0.16[b]
CaZSM5(38)	37.2	72.5	2.0	0.70[c]
CaZSM5(25)	55.6	120.7	2.2	0.74[c]

[a] Calculation based on Ca^{2+} cation in the main channel (site IV).
[b] Calculation based on Ca^{2+} cation in the supercage (site II).
[c] Calculation based on all Ca^{2+} cation.

4. Discussion

4.1. Effect of electrostatic field for reactants adsorption

In dried sodium and calcium exchanged Y zeolites, only 50–60% of the cations are located at site II, which is accessible to adsorbed molecules like propane [8,22]. For mordenite, the occupation of cation in the five types of sites depends on the Si/Al ratio. For MOR with Si/Al ratio of 10 each unit cell contains three sodium cations located at site I (in side channel) and two sodium cations occupying site IV (in the intersection between inside eight-ring and main channel) [23]. The side channels are accessible only to small molecules like methane and oxygen. Larger hydrocarbons, like propane only access the main channels [24].

This study shows that oxygen adsorption can be observed at room temperature in the infrared spectra between 1550 and 1555 cm^{-1} for calcium exchanged Y, MOR and ZSM5 zeolites (Fig. 2). Study of oxygen adsorption on alkaline-earth exchanged Y zeolite revealed that oxygen could adsorb on alkaline-earth cation site via electrostatic interaction to form $M^{2+}(O_2)$ species on the supercage Ca^{2+} cations [16,25]. The dipole-induced polarization of oxygen by the cation electrostatic field results in an infrared active stretch vibration. It was shown that intensity and frequency increased with higher electrostatic field of the cation. The side bands observed at 1570 cm^{-1} and 1542 cm^{-1} (Fig. 2) were attributed to a combination of the O–O stretching vibration with a low-frequency motion of the molecule in its site, as proposed for oxygen adsorbed on CaA [17,18]. From Fig. 3 we can conclude that Ca^{2+}

cations in MOR and ZSM5 have a similar environment as cations in CaY to form $Ca^{2+}(O_2)$ species.

As pointed out in Section 1, the zeolites exhibit different cation positions. Only one site of Ca^{2+} cations in ZSM5 (site I) and Y zeolite (site II) (Fig. 1) are accessible to oxygen [14,26], while in MOR, oxygen can adsorb on Ca^{2+} at both sites I and IV [24]. The electrostatic field of Ca^{2+} in the small side pocket (site I) is shielded stronger than in the main channel (site IV). Consequently, the infrared spectrum showed two $Ca^{2+}(O_2)$ species at 1554 cm^{-1} and 1550 cm^{-1}, which can be attributed to oxygen adsorbed on Ca^{2+} at site IV and site I respectively (Fig. 3). Further, for MOR the Ca^{2+} cations are distributed over site I and site IV exclusively, while in CaZSM site I is occupied for 90% [23]. However, for CaY zeolite approximately 50% of the total Ca^{2+} is located at site II in the supercage [8]. Since also the Ca^{2+} cation concentration varied with Si/Al ratio in the different types of zeolite, the infrared spectra after oxygen adsorption are normalized per Ca^{2+} based on the amounts of Ca^{2+} at the accessible sites (Fig. 7). Clearly, the electrostatic field per accessible Ca^{2+} is the lowest in CaY (multiplied by 2 in Fig. 7). In addition, the electrostatic field in CaZSM5 is much higher than in MOR and Y. This is in agreement with CO adsorption results on different type of Ba^{2+} exchanged zeolites as published by Panov et al. [6]. Compared to CaY and CaMOR, the unusual high electrostatic field of CaZSM5 can be attributed to the fact that Ca^{2+} locates at the isolated aluminum occupied oxygen tetrahedral sites with single negative charges due to high Si/Al ratios (25 or 38). This results in the formation of sites with only partially compensated excessive positive charges of Ca^{2+} [27,28].

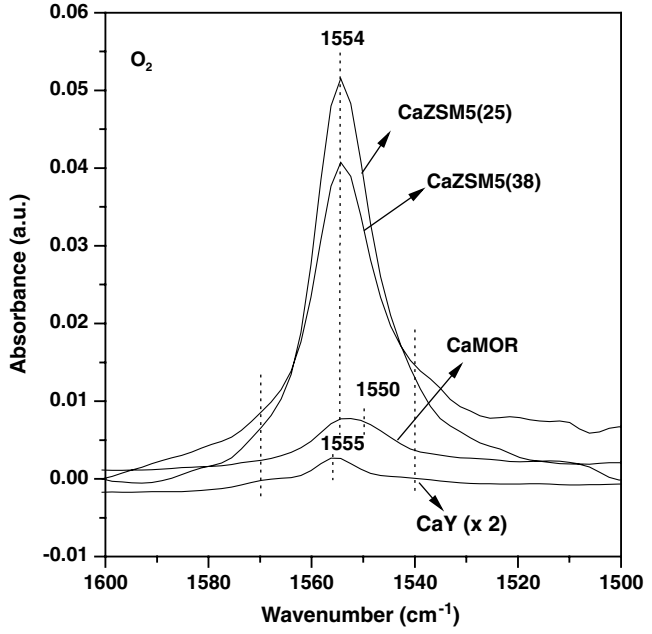

Fig. 7. Normalized infrared spectra of oxygen adsorption at 40 mbar on Ca^{2+} exchanged zeolites. (Normalization based on the effective Ca^{2+} concentration in each zeolite. For example, only Ca^{2+} cation in the supercage for CaY; all Ca^{2+} cation for CaMOR and CaZSM5.)

Recent simulations and experiments showed that propane, at low coverage, mainly adsorbed at supercage cation site in Ca-exchanged Y zeolite [8,13,22]. Experiments with $CH_3CD_2CH_3$ allowed us to make distinction between the IR bands of the methyl groups versus the methylene group; it appeared that the symmetric vibration of both methyl groups shift equally and significantly as compared to gas phase propane. From this we concluded that the Ca^{2+} ion was large enough to allow both propane methyl groups to attach to Ca^{2+}, resulting in the formation of a cyclic geometry. These data are not shown and subject of a submitted publication. Similar to the oxygen adsorption, the interaction between Ca^{2+} and the propane methyl groups is electrostatic in nature. As a result, the Ca^{2+} induced polarization results in a shift of the symmetric stretching vibration of the propane methyl groups to lower frequency (2838 cm^{-1}) with increasing cation electrostatic field [13].

Below 0.2 mbar equilibrium partial pressure, the propane adsorption spectra on CaY, CaMOR and CaZSM5 show similar features (Fig. 4), which suggest that adsorbed propane at the Ca^{2+} sites in all three zeolites exhibits the same cyclic structure. Clearly, with increasing electrostatic field (CaY < CaMOR < CaZSM5), the symmetric stretching vibration frequency of the propane methyl groups moved to lower wave number in the order CaY (2838 cm^{-1}) > CaMOR (2829 cm^{-1}) > CaZSM5 (2826 cm^{-1}) (Fig. 4).

Since CaMOR and CaZSM5 contain much less cations per unit cell than CaY and have higher electrostatic field resulting in stronger adsorption, propane saturates all accessible Ca^{2+} sites in MOR and ZSM5 at lower propane partial pressure compared to CaY. As a result, with increasing propane partial pressure (>0.2 mbar) propane filled the zeolite pores via a dispersive force interaction with the zeolite framework oxygen atoms. As a consequence, the methyl groups are hardly affected by the cation electrostatic field and a peak appeared at 2875 cm^{-1} (Fig. 4), which can also be found in the gas phase propane spectrum.

Since the symmetric CH_3 vibration at 2838–2826 cm^{-1} arises from the $Ca^{2+}(C_3H_8)$ complex, the integrated area of this peak per effective Ca^{2+} site represents the normalized amount of propane adsorbed on Ca^{2+}. The effective number of accessible Ca^{2+} sites for propane was calculated based on the fact that on CaY and ZSM5, the oxygen adsorption sites of Ca^{2+} are also accessible for propane. But on CaMOR, only site IV is accessible for both oxygen and propane; site I adsorbs only oxygen, because propane (0.43 nm) is too large to enter the side pocket (0.26×0.37 nm) (Fig. 1) [23,24]. The thus normalized propane adsorption isotherms of Ca^{2+} exchanged zeolites at room temperature are presented in Fig. 8. Indeed, propane saturated the accessible Ca^{2+} sites on MOR and ZSM5 at much lower pressure than on CaY, where full coverage was not reached even at 1 mbar of propane pressure. From this, it can be concluded that the strength of adsorption increased from CaY to CaMOR to CaZSM5. Further,

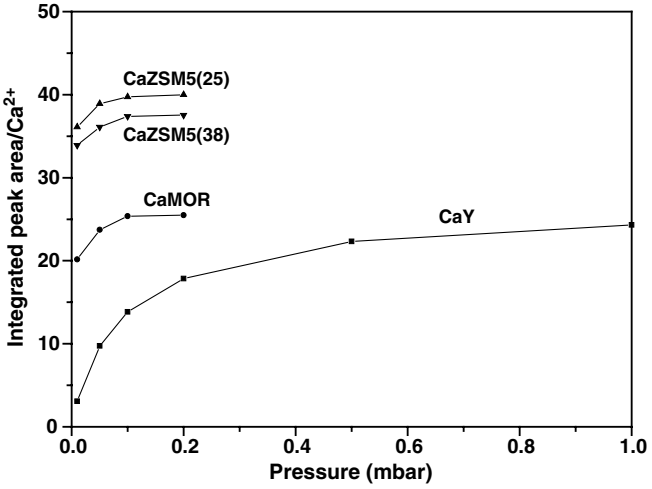

Fig. 8. Propane adsorption isotherms on Ca^{2+} exchanged zeolites at room temperature. Propane adsorption was expressed as integrated area of infrared band at 2838–2826 cm^{-1} per effective Ca^{2+} sites in each zeolite. The effective Ca^{2+} sites used in calculation are Ca^{2+} cation in the supercage (site II) for CaY, in the main channel (site IV) for CaMOR and all Ca^{2+} cation for CaZSM5 (see text for details).

the normalized integrated peak area was found to decrease in the order CaZSM5(25) > CaZSM5(38) > CaMOR > CaY, which can be attributed to the decreasing electrostatic field in the samples, which affects the extinction coefficient of the vibration. These results are in full agreement with the electrostatic field deduced from the oxygen adsorption experiments as shown in Fig. 7.

4.2. Effects of zeolite topology and Brönsted acid concentration on the reaction mechanism

In this study, on CaY zeolite high selectivity to acetone was observed in propane selective oxidation. The 2:1 mixture of 2-propanol to acetone observed on CaZSM5 points to a typical homolytic peroxide decomposition, followed by a radical reaction pathway similar to alkane auto-oxidation reactions [4]. Interestingly, CO_x was observed for CaMOR, in addition to small amounts of acetone and water. These results clearly show that the type of zeolite has a large influence on the mechanism of propane oxidation.

Ca^{2+} sites at the supercage in CaY zeolite is able to adsorb more than one molecule N_2 or CO in a so-called geminal structure via electrostatic interaction [29,30]. When adding propane to CaY pre-covered with oxygen (Fig. 3), the sidebands disappear and the main peak shift to lower frequency and decreased in intensity. These data are not shown here and have been submitted for publication elsewhere. These results strongly suggest that propane and oxygen simultaneously adsorb at the supercage Ca^{2+} site to form $Ca^{2+}(O_2)(C_3H_8)$ species via electrostatic interaction. Consequently, both molecules are activated by the polarization effect induced by the electrostatic field of Ca^{2+}, and their close proximity facilitates reaction [17,30]. The similar propane and oxygen adsorption infrared spectra observed for the three types of Ca^{2+} exchanged zeolites (Y, MOR and ZSM5) (Figs. 3 and 4) in this study suggest that propane and oxygen adsorption results in similar $Ca^{2+}(O_2)(C_3H_8)$ complexes which react to form isopropylhydroperoxide (IHP) [1,5,7,8,13].

Decomposition of IHP studied on CaY showed two parallel pathways. First, heterolytic elimination of water from IHP at Brönsted acid sites is the major path to result in acetone [1]. Second, homolytic decomposition of IHP at the Ca^{2+} site yields $C_3H_7O^*$ and HO* radicals which recombine with propane into two molecules of 2-propanol [13]. In the latter case, Ca^{2+} acted as a Lewis acid center to activate the O–O bond in IHP. The low amount of 2-propanol observed on CaY shows that its low electrostatic field is not capable to induce homolytic splitting of IHP to a large extent.

In contrast to CaY, on CaZSM5 homolytic decomposition of IHP showed to be an important reaction as reflected in the high amount of 2-propanol (Table 2). A 2:1 ratio of 2-propanol to acetone is also found in alkane auto-oxidation reactions [4]. This suggests that in CaZSM5 acetone and 2-propanol both are produced from the homolytic decomposition of IHP, initiated by the high electrostatic field of the charge compensating cations. Since this reaction occurs inside the zeolite channels, radical combination reactions are very limited due to the restricted space. As a result no other radical combination products (e.g. ester) have been observed. As discussed in the previous section, Ca^{2+} cations in ZSM5 are located at isolated aluminum sites with single negative charges, resulting in cation sites that only partially compensate the positive charge on a Ca^{2+} cation. Those Ca^{2+} cations possess unusually high Lewis acidity, which results in strong activation of the IHP O–O bond, followed by homolysis. Moreover, IHP decomposition to acetone occurs at Brönsted acid sites. Protons are normally located at the zeolite framework oxygen site next to the aluminum. However, the isolated Al sites in the high Si/Al ratio ZSM5 zeolites prevent the IHP at Ca^{2+} sites to diffuse easily to the proton sites. In addition, CaZSM has much less Brönsted acid sites compare to CaY (Fig. 2), which again favors the IHP homolytic decomposition. Finally, the high amount of propane adsorbed in the ZSM5 zeolite pores contributes to a higher rate of 2-propanol formation.

Comparison of the total acetone and 2-propanol production per Ca^{2+} cation site on CaY and CaZSM5 (Table 2) reveals that Ca^{2+} in CaZSM5(25) is about five times more active than in CaY (Table 2). Again, this is attributed to the very high electrostatic field of Ca^{2+} in ZSM5. With increasing Si/Al ratio of ZSM5, the total amount of acetone and 2-propanol per Ca^{2+} cation decreased slightly, because of the lower field in ZSM5(38). Clearly, the 2-propanol to acetone ratio decreased dramatically with the stronger decreasing electrostatic field from CaZSM5 to CaY.

Although propane and oxygen adsorption showed a reasonable electric field of Ca^{2+} in CaMOR, low acetone formation was observed on CaMOR. Moreover, total oxidation to CO_x was found. Over-oxidation of acetone was excluded, since no further oxidation occurred in the

presence of acetone and oxygen at 353 K. We suggest that the full oxidation of propane is due to the location Ca^{2+} in the unique one-dimensional channel structure together with the high Brönsted acid concentration. As discussed above, in MOR, only Ca^{2+} at site IV (Fig. 1b) is accessible to both propane and oxygen molecules to allow reaction. The unique one-dimensional channel (0.65×0.7 nm diameter) in MOR seems to inhibit the formation of the branched IHP molecule at the Ca^{2+} site. Consequently, only minor amounts of acetone were found. On the other hand, acidic zeolites are well known as cracking catalyst for hydrocarbon molecules [15]. The high Brönsted acid concentration and the highly polarized propane molecule in CaMOR could induce propane cracking. In the presence of oxygen, the cracking intermediates (e.g. radicals or carbocation) may further oxidize to CO and CO_2. Cracking is most likely inhibited in lower acidic zeolites such as CaY and CaZSM5. Further, although ZSM5 has small channels with diameter of 0.53×0.56 nm in case of the straight channels and 0.51×0.5 nm in case of the sinusoidal channels, preferential location of Ca^{2+} is at the intersections of both channels (Fig. 1c) providing enough space to accommodate IHP. Also the supercage in zeolite Y is large enough (Fig. 1a) to allow propane selective oxidation.

In good agreement with our previous results, this study confirmed that a high electrostatic field of Ca^{2+} determines the propane oxidation activity and selectivity to partially oxidized products that are strongly adsorbed in the zeolites. However, it also became clear that the geometrical restrictions affect the activity due to the limitation of formation transition-state complexes to IHP at Ca^{2+}. The optimal ratio between Brönsted acid sites and Ca^{2+} cation could enhance reaction activity, but too high concentration of Brönsted acid sites also affects selectivity due to hydrocarbon cracking.

5. Conclusions

Based on oxygen and propane adsorption at room temperature, the electrostatic field of Ca^{2+} was observed to increase in the order CaY < CaMOR < CaZSM5(38) < CaZSM(25). The electrostatic field and Lewis acidity of Ca^{2+} cations in CaY and CaZSM5 was found to correlate with activity and selectivity of the surface reaction of propane selective oxidation. At 353 K, low activity but high selectivity to acetone was observed for propane oxidation on CaY zeolite due to heterolytic H_2O elimination of reaction intermediate IHP. On CaZSM5, an unusual high electrostatic field and Lewis acidity of Ca^{2+} cation resulted in high activity, but favored homolytic IHP decomposition, which formed a 2:1 mixture of 2-propanol and acetone in the products. On CaMOR, the steric restriction for accommodating the transition-state complex to IHP resulted in the lowest activity of acetone formation. Furthermore, the high Brönsted acid concentration with high propane polarization on CaMOR resulted in propane deep oxidation to form CO and CO_2. It is convincingly shown that the electrostatic field of Ca^{2+}, the zeolite structures and the presence of Brönsted acid sites determine the reaction paths in propane partial oxidation on Ca^{2+} exchanged zeolites.

Acknowledgements

This work was performed under the auspices of The Dutch Institute for Research in Catalysis (NIOK). We thank J.A.M. Vrielink for XRF measurements and B. Geerdink for technical support. Financial support from CW/STW Project No. 790-36-057 is gratefully acknowledged.

References

[1] J. Xu, B.L. Mojet, J.G. van Ommen, L. Lefferts, Phys. Chem. Chem. Phys. 5 (2003) 4407.
[2] Y. Xiang, S.C. Larsen, V.H. Grassian, J. Am. Chem. Soc. 121 (1999) 5063.
[3] D.L. Vanoppen, D.E. De Vos, P.A. Jacobs, Prog. Zeolite Micropor. Mater., Pts A–C 105 (1997) 1045.
[4] D.L. Vanoppen, D.E. De Vos, P.A. Jacobs, J. Catal. 177 (1998) 22.
[5] H. Sun, F. Blatter, H. Frei, Catal. Lett. 44 (1997) 247.
[6] A.G. Panov, R.G. Larsen, N.I. Totah, S.C. Larsen, V.H. Grassian, J. Phys. Chem. B 104 (2000) 5706.
[7] F. Blatter, H. Sun, S. Vasenkov, H. Frei, Catal. Today 41 (1998) 297.
[8] J. Xu, B.L. Mojet, J.G. van Ommen, L. Lefferts, J. Phys. Chem. B 108 (2004) 15728.
[9] J.L. Schlenker, J.J. Pluth, J.V. Smith, Mater. Res. Bull. 14 (1979) 751.
[10] L.M. Kustov, V.B. Kazansky, J. Chem. Soc. Faraday Trans. 87 (1991) 2675.
[11] S. Bordiga, E. Garrone, A. Lamberti, A. Zecchina, V.B. Kazansky, L.M. Kustov, J. Chem. Soc. Faraday Trans. 90 (1994) 3367.
[12] T. Ohgushi, T. Niwa, H. Arakia, S. Ichino, Micropor. Mesopor. Mater. 8 (2004) 231.
[13] J. Xu, B.L. Mojet, J.G. van Ommen, L. Lefferts, J. Catal. 232 (2005) 411.
[14] D.W. Breck, Zeolite Molecular Sieves: Structure, Chemistry, and Use, Wiley, New York, 1974, p. 464.
[15] H. van Bekkum, Introduction to Zeolite Science and Practice, Elsevier, Amsterdam, 2001, p. 371.
[16] G.H. Smudde, T.L. Slager, S.J. Weigel, Appl. Spectrosc. 49 (1995) 1747.
[17] J. Xu, B.L. Mojet, J.G. van Ommen, L. Lefferts, J. Phys. Chem. B 109 (2005) 18361.
[18] F. Jousse, E.C.D. Lara, J. Phys. Chem. 100 (1996) 233.
[19] K.M. Gough, W.F. Murphy, J. Phys. Chem. 87 (1987) 3332.
[20] J.N. Gayles, W.T. King, Spectrochem. Acta 21 (1965) 543.
[21] G. Socrates, Infrared and Raman Characteristic Group Frequencies: Tables and Charts, Hone Wiley & Sons, 2001, p. 302.
[22] S. Calera, D. Dubbeldam, R. Krishna, B. Smit, T.J.H. Vlugt, J.F.M. Denayer, J.A. Martens, T.L.M. Maesen, J. Am. Chem. Soc. 126 (2004) 11377.
[23] M. Rep, A.E. Palomares, G. Eder-Mirth, J.G. van Ommen, N. Rosch, J.A. Lercher, J. Phys. Chem. B (104) (2000) 8624.
[24] E. Beerdsen, B. Smit, S. Calera, J. Phys. Chem. B 106 (2002) 10659.
[25] K.M. Bulanin, K.L. Lobo, M.O. Bulanin, J. Phys. Chem. B 104 (2000) 1269.
[26] I.G. Bajusz, J.G. Goodwin, Langmuir 14 (1998) 2876.
[27] V.B. Kazansky, A.I. Serykh, Phys. Chem. Chem. Phys. 6 (2004) 3760.
[28] V.B. Kazansky, A.I. Serykh, Micropor. Mesopor. Mater. 70 (2004) 151.
[29] K. Hadjiivanov, E. Ivanova, H. Knozinger, Micropor. Mesopor. Mater. 58 (2003) 225.
[30] K. Hadjiivanov, E. Ivanova, D. Klissurski, Catal. Today 70 (2001) 73.